Ocean circulation over the Saya de Malha Bank in the South West Indian Ocean

Priscilla Coopen[1]*, Yuneeda B. N. Oozeeraully[1], Marek Ostrowski[2]

[1] Department for Continental Shelf, Maritime Zones Administration and Exploration, Prime Minister's Office, Belmont House 2nd Floor, Intendance Street, Port Louis, 11328, Republic of Mauritius

[2] Institute of Marine Research (IMR), PO Box 1870 Nordnes, N-5817 Bergen, Norway

* Corresponding author: pcoopen@govmu.org

Abstract

The Saya de Malha Bank is one of the major banks of the Mascarene Plateau in the South West Indian Ocean. It is known for its unique ecosystem, remoteness (nearest island is about 300 km away) and complex oceanographic conditions. This study presents the results of a survey conducted in May 2018 on-board the R/V Dr Fridtjof Nansen, and aims to provide a descriptive overview of the interaction of the large-scale South Equatorial Current (SEC) over the shallow Saya de Malha Bank. The analysis of the current pattern revealed a two-layered structure of the current over the shallow topography of the bank compared to the vertically rigid-structure of the SEC throughflow in its deeper region. This two-layered flow consists of a surface layer and a sub-thermocline layer. The top layer flow, carrying the lower salinity mass (Tropical Surface Water) is driven by the Ekman dynamics observed in the southern hemisphere whereas the sub-thermocline current layer is most likely governed by the tidal and internal wave dynamics generated by the topographic relief of the bank.

Keywords: Saya de Malha Bank, South Equatorial Current, thermocline, Mascarene Plateau, ocean circulation

Introduction

The tropical south Indian Ocean is characterized by the large-scale circulation called the South Equatorial Current (SEC), which is a major westward current in the latitude band between 10° to 20°S and is most intense at the surface, reaching a depth of 1400 m (Schott and McCreary, 2001; New *et al*., 2007; New *et al*., 2005). When the SEC meets the Mascarene Plateau, an arch-shaped submarine ridge comprising of a series of shallow banks (Cargados Carajos Bank, Nazareth Bank, Saya de Malha Bank and Seychelles Bank) that rise sharply from the deep ocean in the South West Indian Ocean (SWIO), it has a profound effect on the basin-scale current system (Schott and McCreary, 2001).

The overall effect of the Mascarene Plateau is to split the SEC into two cores, forming the northern and southern cores of the SEC downstream of the plateau and the current is forced to follow the bathymetric contours of the banks (New *et al*., 2007) which are eventually funnelled across to the SWIO through the gaps found between the shoals of the plateau (New *et al*., 2007; Vianello *et al*., 2017). Most of the SEC flows through three gaps (channels): between Seychelles and the Saya de Malha Banks; between the Saya de Malha and Nazareth Banks; and between Cargados Carajos Bank and Mauritius island. The volume transported in these gaps varies due to the varying influence of the two monsoon seasons (northeast Monsoon and southwest Monsoon) on the SEC (Vianello *et al*., 2017). In addition, the interaction of incident currents with the abrupt topographical changes prompts local oceanographic conditions to support the formation of unique mid-ocean shallow sea ecosystems (Genin, 2004; Payet, 2005).

The SEC also acts as a barrier in the upper ocean between water masses of southern and northern origins (Schott and McCreary, 2001; New *et al.,* 2007; New *et al.,* 2005). For instance, the Subtropical Surface Water (STSW), Sub-Antarctic Mode Water (SAMW)

http://dx.doi.org/10.4314/wiojms.si2021.2.1

and Antarctic Intermediate Water (AAIW) are present on the southern side of the SEC as compared to the Arabian Sea High Salinity Water (ASHSW) and Red Sea Water (RSW) on its northern side (New *et al.,* 2007). Tropical Surface Water (TSW) is also evident as a fresh surface layer which is carried westward by the SEC in the upper 50–100 m. At deeper depths, the North Indian Deep Water (NIDW) and Antarctic Bottom Water (AABW) are found to the west of the Mascarene Plateau (New *et al*., 2007; Pous *et al*., 2014). The SEC therefore forms a sharp boundary between the subtropical water masses from further north (nutrient-rich waters) and south (nutrient-poor waters) of the bank (New *et al*., 2007; Vortsepneva, 2008). The interaction of the SEC with the Mascarene Plateau further plays a significant role in the supply of water masses to the SWIO (New *et al.*, 2005; New *et al.*, 2007; Vianello *et al.*, 2017).

The Saya de Malha Bank is one of the major banks of the Mascarene Plateau and has an area of about 40, 808 km^2 (Vortsepneva, 2008), and is comprised of the smaller Ritchie Bank and the South Bank. This paper focuses on the latter which will be hereafter referred as Saya de Malha (SDM). The SDM has been the target of various scientific research works during recent years due to the uniqueness of its ecosystems (Bergstad *et al.,* 2021; Ramah *et al.,* 2022), the complexity of its oceanographic processes (da Silva *et al.*, 2011; New *et al.*, 2013; Lindhorst *et al*., 2019) as well as its geological nature and biogeochemistry (Lindhorst *et al.,* 2019). The oceanographic conditions that develop over SDM and their impact on local biological productivity are strongly influenced by a superposition of the steady SEC flow with barotropic tides (da Silva *et al.*, 2015) upon interacting with the relief of the bank. As a result of these interactions, barotropic tidal energy is transferred to internal solitary waves (ISWs) at the southern end of the bank, which propagate towards the shallow bathymetry where they break (New *et al.*, 2013). The ISW breaking induces turbulence and intense mixing, which appears to boost nutrient supply and chlorophyll production in otherwise oligotrophic environments (New *et al.*, 2013; Ostrowski *et al.*, 2009; Zeng *et al.*, 2021).

In May 2018, the Norwegian research vessel, R/V Dr Fridtjof Nansen, in collaboration with the Mauritius and Seychelles Joint Management Authority, conducted a survey over the SDM that lasted almost three weeks. It is to be noted that the SDM is within the Joint Management Area and is jointly managed by both the Republic of Mauritius and the Republic of Seychelles under the Joint Management Treaty (Treaty Concerning the Joint Management of the Continental Shelf in the Mascarene Plateau Region - CLCS, 2011). The aim of the survey was to carry out a systematic study of the benthic ecosystems and morphology of the bank. The survey covered the entire area of the bank with an adequate spatial resolution with the vessel-mounted Acoustic Doppler Current Profiler (ADCP) operated continuously underway. In this paper, the collected ADCP data were used to provide a general description of the circulation over the inner sections of SDM and its connection to the SEC throughflow along the southern slopes in May 2018.

Materials and methods

Study area

The SDM is a large bank with a summit surface of about 350 km wide (Kara and Sivuka, 1990) and is located between latitudes 10-13°S and longitudes 59.30-62.30°E as shown in Figure 1a. The closest land, the Agalega Island, is approximately 300 km away. The bank is about 900 km and 700 km south of Mauritius and north of Seychelles, respectively. It is separated from the Nazareth Bank, in the south, by a 1100 m deep channel. The bank experiences relatively steady southeast trade winds. During the southern winter, the northern edge of the trade winds shifts northward and falls during the southern summer and autumn (Schott *et al.*, 2009). The precipitation in the region is around 100-200 mm/month during December, January and February and less than 50 mm/month during June, July and August (Schott *et al.*, 2009).

Survey approach

The field survey was undertaken on board the R/V Dr Fridtjof Nansen (Survey no. 2018406) (Bergstad *et al*., 2020) in May 2018 just before the onset of the southwest Monsoon season. The survey approach was derived primarily to characterize the marine ecosystem and morphology of SDM. It consisted of two legs as shown in Figure 1 (b and c). Leg 1 followed a pre-determined trajectory of eight parallel transects covering the whole bank. Each transect was separated by approximately 15 nautical miles from the other and covered the entire width of the bank from its western to its eastern edge, extending a few miles into the surrounding deep ocean. Leg 2 involved an intense sampling programme for habitat mapping at selected locations and did not follow a fixed transect grid. At the end of Leg 2, the vessel concluded the observations over the bank and departed southwards, crossing the SN sill towards the Nazareth Bank.

Ship-based ADCP data

Ocean current velocities and directions were recorded and measured continuously while the ship was underway with the vessel-mounted Ocean Surveyor 75 kHz and 150 kHz Acoustic Doppler Current Profiler (ADCP) by the Teledyne RD Instrument (RDI). The 75 kHz ADCP has a vertical resolution of 16 m and maximum depth of 800 m. The respective values for 150 kHz units were 8 m and 300 m.

CTD and wind data

The vertical profiles of temperature, salinity and dissolved oxygen were determined using the Seabird 911 plus Conductivity, Temperature and Depth (CTD) profiler. A total of 44 CTD stations covering the full depth of the water column were included in the survey, among which 30 were during Leg 1 (Fig. 1b) and 14 during Leg 2 (Fig. 1c).

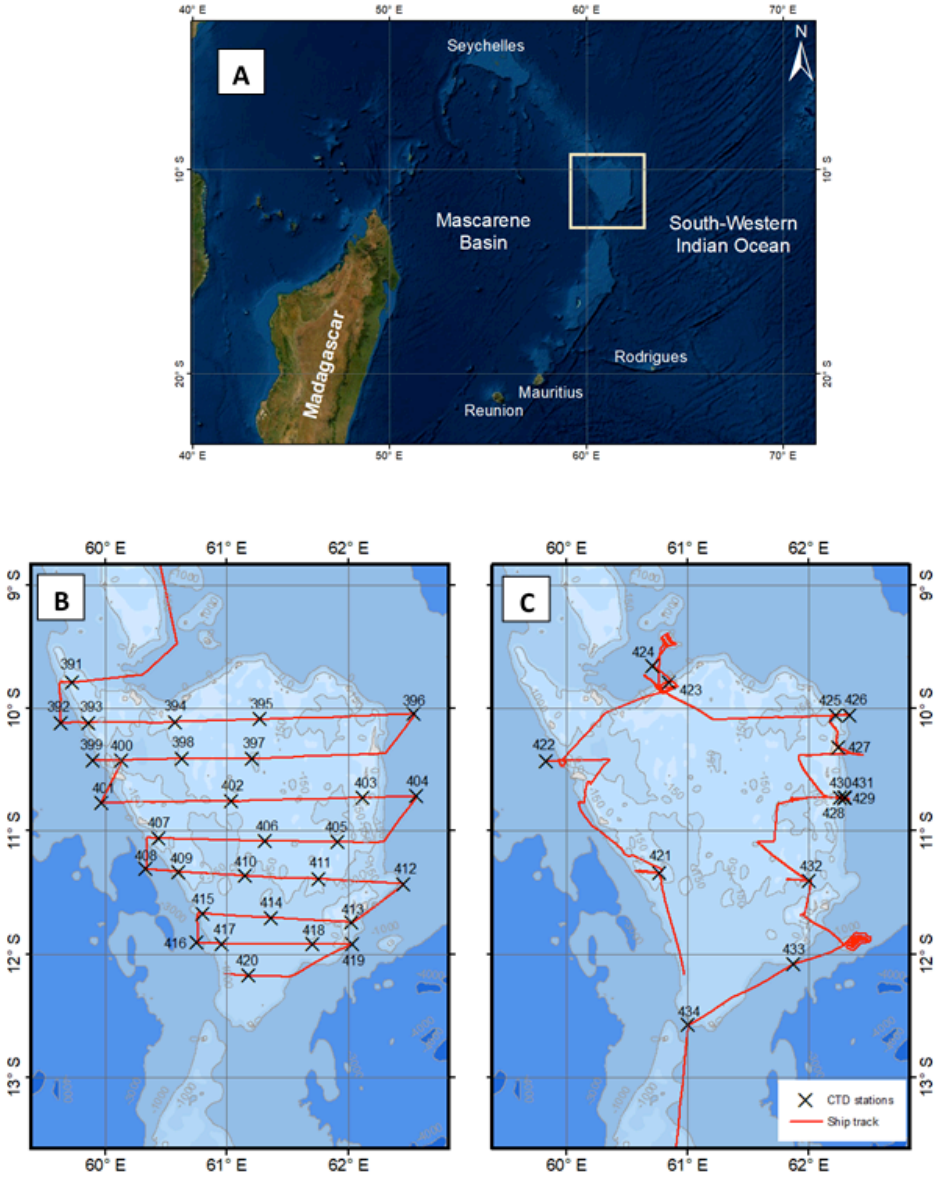

Figure 1. a) Region of the Mascarene Plateau surveyed in May 2018 (yellow box); b) Leg 1 of the survey (7-15 May 2018); and c) Leg 2 of the survey (15-25 May 2018) with their corresponding CTD stations undertaken over the Saya de Malha Bank.

Wind speed and direction data were collected with the vessel's Automated Weather Station (AWS) mounted 10 m above sea level with a sampling rate of 1 minute.

Bathymetry

The bathymetry of SDM was derived by merging the GEBCO 2021 atlas data (https://www.gebco.net) with the shallower depth *in situ* echo-sounding data (less

than 300 m deep) from 2008 (Stømme *et al*., 2009) and 2018 (Bergstad *et al*., 2020) Nansen expeditions.

Satellite data

The daily satellite data from the GlobCurrent product were used in this study. The images for the observational period from 7-27 May 2018 were accessed through the Copernicus Marine Service website (https://www.copernicus.eu/en), product MULTIOBS_GLO_PHY_REP_015_004. GlobCurrent combines altimetry-derived geostrophic currents and Ekman (wind-driven) currents (Cancet *et al.*, 2019). These data are distributed on a 0.25-degree grid.

Data analysis and techniques

The ADCP data were processed using a version of OSSI post processing software developed at GEOMAR (Fischer *et al.*, 2003) and adapted to the specifics of fishery surveys at the Institute of Marine Research, Norway [Ostrowski, personal communication]. The pre-processing involved removing erroneous data, bottom masking, and correcting the misalignment between the ship and the ADCP beam axis. The misalignment angle and its standard error were estimated to be -0.25° and 0.006° for the 150 kHz and 0.06° and 0.006° for the 75 kHz ADCP. As a result of this analysis, a time-averaged dataset with a 2-minute sampling step was obtained.

In this study, the 150 kHz data were used in the inner part of SDM, whereas the 75 kHz result was utilized exclusively to compute transports in the southern section of the bank and across the SN sill. The volume transport was computed using the following equation:

$$Volume\ transport = \iint v.dA$$

where v is the velocity and dA is the area normal to the velocity.

The vertical shear squared (Sh^2) of the horizontal velocity was computed using the following equation:

$$Sh^2 = (\frac{\partial u}{\partial z})^2 + (\frac{\partial v}{\partial z})^2$$

where $(\frac{\partial u}{\partial z})^2$ and $(\frac{\partial v}{\partial z})^2$ represent the contribution of the vertical shear associated with the zonal and meridional currents respectively.

The CTD data were quality checked and erroneous data and spikes were removed. The postprocessing was carried out using the Seasave software from Sea-Bird Scientific. The salinity and oxygen data were validated on-board by comparison with water bottle samples using the Guildline Portasal 8410A and the Winkler method (Langdon, 2010), respectively. The dual sensor configuration on the CTD probe secured the validation of temperature data.

The raw data of wind speed and direction displayed numerous gaps. After the removal of these gaps, the valid data sections were low-pass filtered using a 15-minute lag. Finally, the filtered dataset was regularised on a grid with a cell resolution of 10 x10 km to account for overlapping coverage when the ship was manoeuvring.

Results

Topographic features of Saya de Malha Bank

The overall topographic architecture of the bank can be divided into three main parts: a shallow submerged reef rim surrounding the eastern and northern part of the bank with a bathymetry of less than 40 m deep; an interior central lagoon (CL) of 70-150 m deep which opens up in the south shelf break ledge (SBL) of the bank at depths between 200 to 250 m; and a narrow southern tip (South Point - SP) with depth greater than 250 m. Moving from the west to east of the plateau (Fig. 2a), the water depth on the western part of the bank is around 70 m, in the lagoon (CL) 120 m and about 40 m in the eastern part (ES). This indicates that the plateau on the eastern side is more elevated than on the western side. Surrounding the eastern (ER) and northern rims (NR) are shallow areas of 40 to 100 m deep. The interior part of the bank consists of pinnacles and/or local highs protruding from the seafloor. One of them can also be seen on the western side, labelled western tower (WT) and stands about 75 m above the seafloor. Another similar pinnacle is located on the eastern side. It is a stand-alone seamount-type structure (hereafter referred to as the South Bank or SB). The main structures of the bank follows the description presented by Vortsepneva (2008) from the research work done in the 1980s.

Wind conditions

Steady southeasterly wind with velocities ranging between 10-12 m s^{-1} dominated throughout the survey period. The wind velocities however dropped to 7-8 m s^{-1} for a few hours on 14, 17, 20 and 22 May 2018 (not shown). The wind pattern observed on 8 May was an exception as the wind velocities reduced to 3-4 m s^{-1} with the wind direction being predominantly from the northeast. The overall wind conditions observed

over the SDM were consistent with the western Indian Ocean (WIO) wind climatology, characterized by the steady southeast trades south of 10°S (Schott and McCreary, 2001).

Water masses

Figure 3 presents temperature, salinity, and dissolved oxygen sections across the bank, in a north-south direction (Fig. 2b). All distributions showed the same vertical structure, consisting of the top layer of Topical Surface Water (TSW), characterized by uniform temperature (28.2-28.4°C), salinity (31.1-31.4 PSU) and oxygen (4.5-4.6 ml/L) ranges. This fresh TSW layer is transported by the SEC from the western Pacific region (New *et al.*, 2007; Vianello *et al.*, 2017) and was observed throughout the SDM region. The TSW varied across latitudes between depths of 40 to 70 m, with shallower depths in the northern part and deeper depths in the southern part of the bank. At the southern end of the section, the pycnocline was found at 60 m but appeared to shoal northwards. However, at the shallowest station, Sta. 395 located at the northern terrace, stratification was absent as the TSW layer extended to the bottom. Strong stratification separated the top TSW layer from colder, more saline and oxygen-deficient water masses below, identified as the Indonesian Throughflow Water (ITF) and the Subtropical Surface Water (STSW). The vertical profile of dissolved oxygen at Sta. 402 also displayed a low oxygen content (< 2 ml/L) in the Central Lagoon (CL) compared to the surrounding deep ocean, thus indicating higher production and decomposition rates in this region. Therefore, the local oceanographic conditions could be favourable to sustain regional productivity due to the topographic features of the bank. However, given the sparse CTD stations spacing over the Central Lagoon, the above observation is inconclusive.

Satellite observations – surface current pattern

Figure 4 presents streamlines of satellite-derived daily currents over the SDM and SN sill on the first and last day of the survey (on 7 and 27 May, 2018 respectively). The streamlines are overlaid on the shaded bathymetry. The location of the SEC core is manifested by the current velocities exceeding 40 cm s^{-1} (the green hue on the colour scale). Between the start and end of the survey, the flow patterns had evolved visibly. On 15 May 2018, on the eastern (upstream) side, the incident SEC flew in three separate cores (not shown). On 27 May 2018, in contrast, the upstream SEC reformed to a broad current extending from 10° to 14°S and further south. On both days (7 and 27 May 2018), the SEC streamlines behaved similarly – diverging into two branches on the upstream side of SDM; one branch swinging around the southern tip of the bank, the other following along the bank's northern edge. The two branches manifested topographic steering action where geostrophic flows must follow the bottom contours (Cushman-Roisin and Beckers, 2011). With a resolution of 0.25 degree, the GlobCurrent-derived streamlines presented in Figure 4 could only reproduce the largest-scale features of this process.

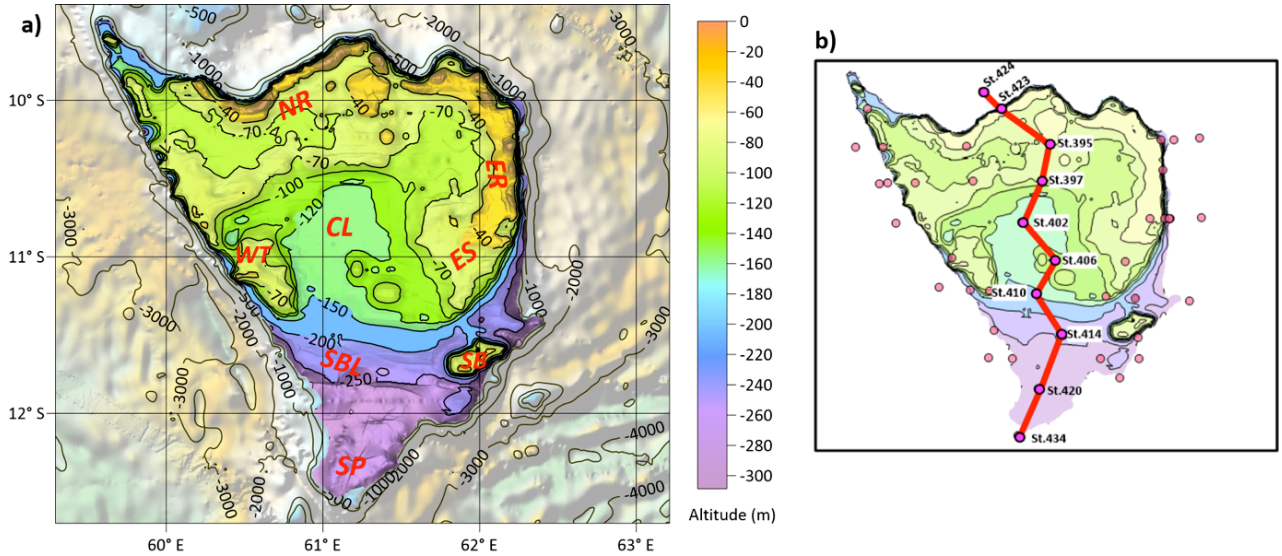

Figure 2. a) Bathymetry of the Saya de Malha Bank's shallow regions (above 300 m): NR – Northern Rim, ER – Eastern Rim, CL – Central Lagoon, ES – Eastern Slope, WT – West Tower, SB – South Bank, SBL – Shelf Break Ledge and SP – South Point; and b) Southbound section (red line) representing CTD stations used for the vertical distribution plots (pink dots represent all CTD stations).

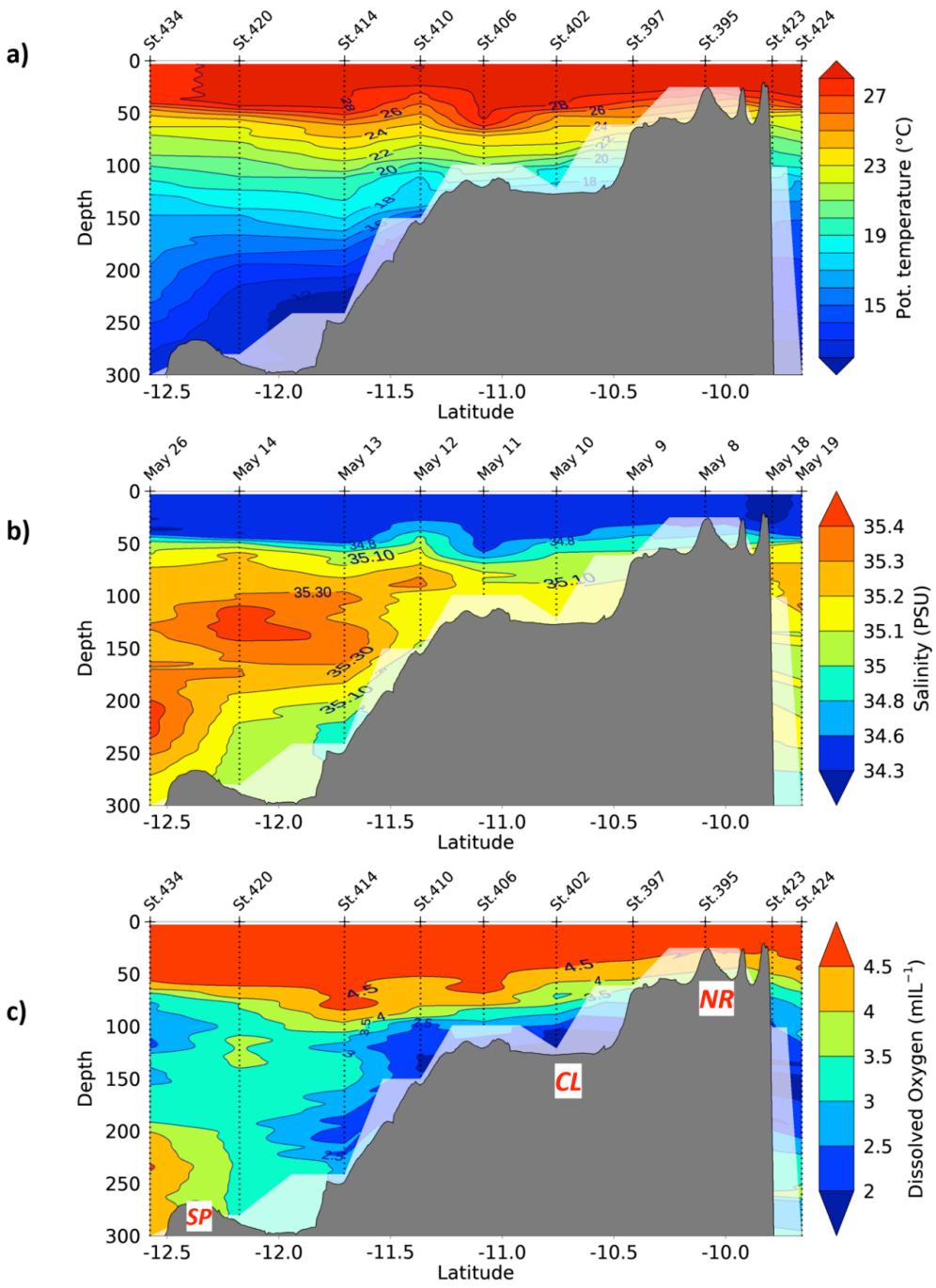

Figure 3. Latitudinal distribution of: a) Potential temperature (°C); (b) Salinity (PSU); and (c) Dissolved oxygen concentration (ml/L) across the Saya de Malha Bank.

ACDP currents

The ADCP data showed similar trend as previously described in the satellite observations; that is, upon reaching the eastern slopes of SDM, the SEC diverges into a northeastward and southwestward direction feeding the northern and southern part of the bank respectively. The ADCP currents revealed a general current pattern in the surface layer across the bank which flowed in a southwestward direction with velocities of 10-20 cm s^{-1} (Fig. 5a) and increasing intensity towards the south of the bank reaching velocities of 40-50 cm s^{-1} (Fig. 6). Furthermore, an eastward current was observed below the surface layer with velocities of 10-20 cm s^{-1}. This two-layered structure of the current was also apparent on the central region of the bank which demonstrates the complexity of the interaction of currents with the mountainous topography of SDM. The intensity of the SEC was found

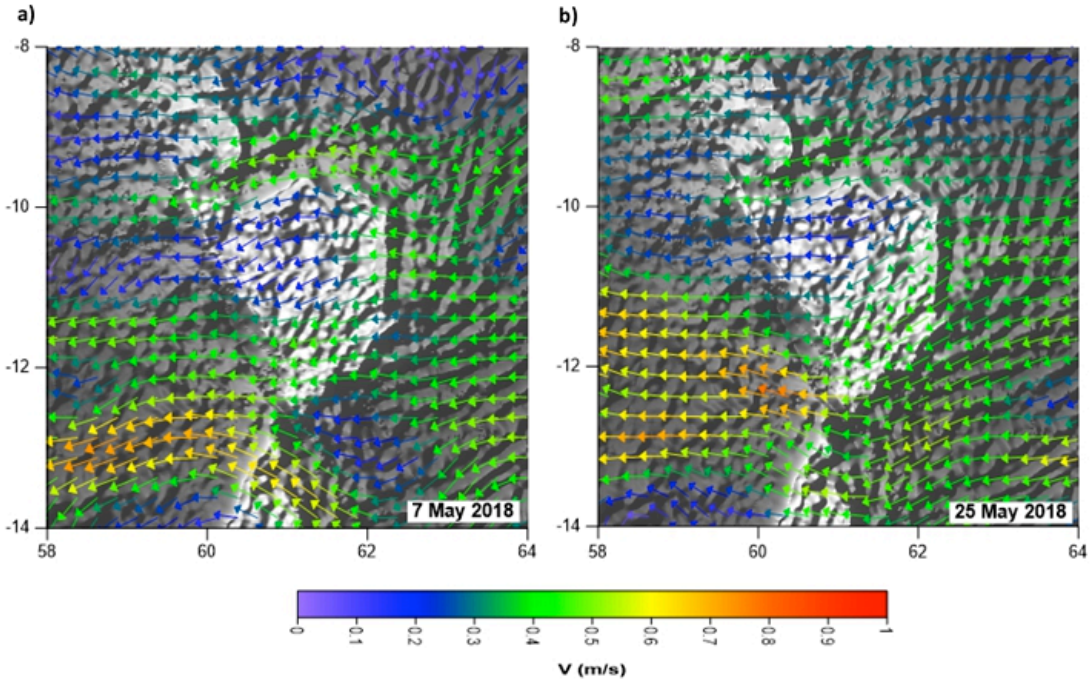

Figure 4. Streamlines of satellite-derived daily surface currents (m s^{-1}) over the Saya de Malha region for: a) 7 May 2018; and b) 25 May 2018.

to be greater at the northeastern and the southern regions of the bank. The southern branch of the current circumvented the Shelf Break Ledge (SBL) and continued westward, joining the SEC flow channelled through the SN sill. The current between latitudes 12° S to 14° S, in the SN sill, reached velocities of between 50-70 cm s^{-1}.

Figure 5 presents the horizontal currents measured over the inner part of SDM for two depth ranges: the 18-26 m, characterizing the top surface layer, TSW transport; and the 58-66 m, associated with the underlying layer, ITF/STSW. Figure 7 enhances this presentation by using the same data to show selected vertical sections of the meridional current component. The first impression from examining these figures is the randomness of the presented current vectors. This appears as a stark contrast to the smooth streamlines of the satellite-derived surface current shown in Figure 4, representing the mesoscale currents as compared to the resolution of the ADCP currents observed over the bank. However, similarities between both the satellite (Fig. 4) and ADCP currents (Fig. 5a) can be distinguished. Firstly, the TSW transport over the inner bank regions (CL, NR, ER; transects 2 to 5) and satellite-derived streamlines shared the same current speed range (10-20 cm s^{-1}) and, generally, the same, southwestward orientation. Moreover, towards the shelf break region (SBL, transect 6), on both figures, the current speed approximately doubled and assumed the direction of bathymetric contours (seawards of 200 m, cf. Fig. 5a and 6a) – manifesting the topographic steering of the SEC southern branch. Lastly, the bifurcation of the incident SEC into the southward and northward branches on the east side of the bank was present on both distributions. The reverse flows along the eastern slope of the bank were clearly identifiable at the ADCP transects 2 and 6 (Fig. 5a; Fig. 7a and c), while the satellite image demonstrated the same process of the SEC bifurcation on the bank's topography at a large scale. Comparing ADCP currents observed above and below the thermocline (Fig. 5a and b), the separation of the flows for the top layer and underlying layer was evident. The top TSW layer over the inner bank evidently followed the southern hemisphere Ekman layer dynamics, deflecting flow to the left of the wind direction. In contrast, the sub-thermocline layer appeared to recirculate around the Central Lagoon (Fig. 5b).

Figure 6a presents the horizontal distribution of ADCP currents from the 42-50 m, thus representing the current at the base of the thermocline (Fig. 3) for the southern region of the bank. The tendency of the flow to follow the 200 m depth contour across Line A and Line B is evident. Figure 6b presents the zonal current across these two lines. The surface-intensified zonal current dominated the observations in the downstream section (Line A, Fig. 6b). The zonal flow

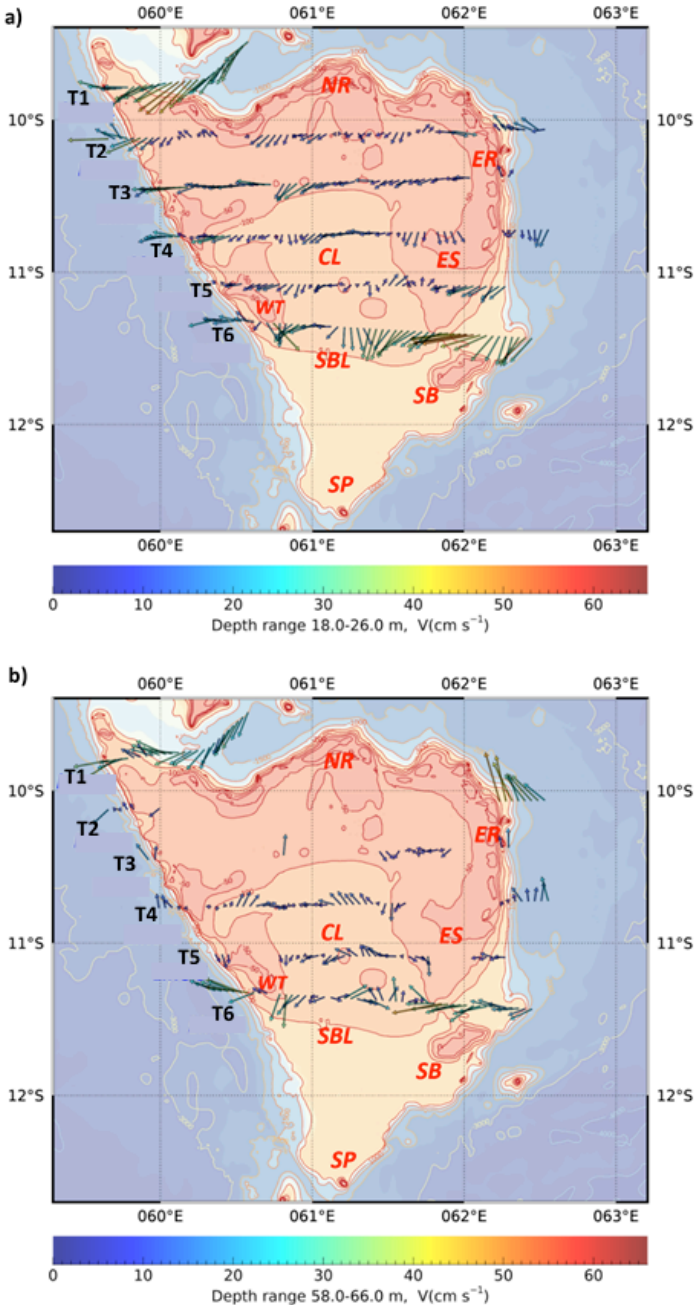

Figure 5. Distribution of ADCP-derived currents (cm s^{-1}) over the Central Plateau and northern perimeter of Saya de Malha Bank for the: a) Surface layer (18-26 m); and b) Sub-thermocline layer (58-66 m).

exceeded 50 cm s^{-1} in the upper layer and decreased gradually with the depth dropping to velocities of 10-20 cm s^{-1} below 200 m. This current flow velocity profile was also observed in the SN sill which was identified as a place of enhanced tidal currents that trigger internal solitary wave packets propagating onto SDM (Konyaev *et al*., 1995; da Silva *et al*., 2011, New *et al*., 2013; da Silva *et al*., 2015).

The upstream section (Line B, Fig. 6b) extended from the South Bank (SB) to the Eastern Slope (ES) and the shallow water of the Eastern Rim (ER) region. The zonal flow, initially barotropic to the south of the SB, over the shallow regions (ER) transformed into a two-layer current. The top and bottom currents were separated at the thermocline depth, hence entrained different water masses, TSW and ITF/STSW, respectively (Fig. 3). According to the presented vertical distribution, the two layers differed in the flow direction. Only the TSW layer displayed the westward zonal drift in contrast to the underlying ITF/STSW. Remarkably, the generally westward zonal current reversed abruptly to

eastward above the pinnacle on the northern side of the channel separating the SB from ES, suggesting a topography forced recirculation – the Taylor Column (Cushman-Roisin and Beckers, 2011).

Volume transport

Although applied to sub-optimal data (as the transects were not designed to provide accurate transport estimates), the volume transport was computed from Lines A and B (Fig. 6a) which produced a plausible result. A total volume transport of 3.88 Sv (Sv = 10^6 m^3 s^{-1}) and 3.44 Sv were computed from Lines A and B respectively. The volume transport for both lines substantiates the topographic steering of the SEC along the southern slope of SDM. The volume transport was also calculated from transect 6 (Fig. 7c) for the sub-thermocline layer resulting in 0.3 Sv (northwards) and -0.28 Sv (southwards) which supports the

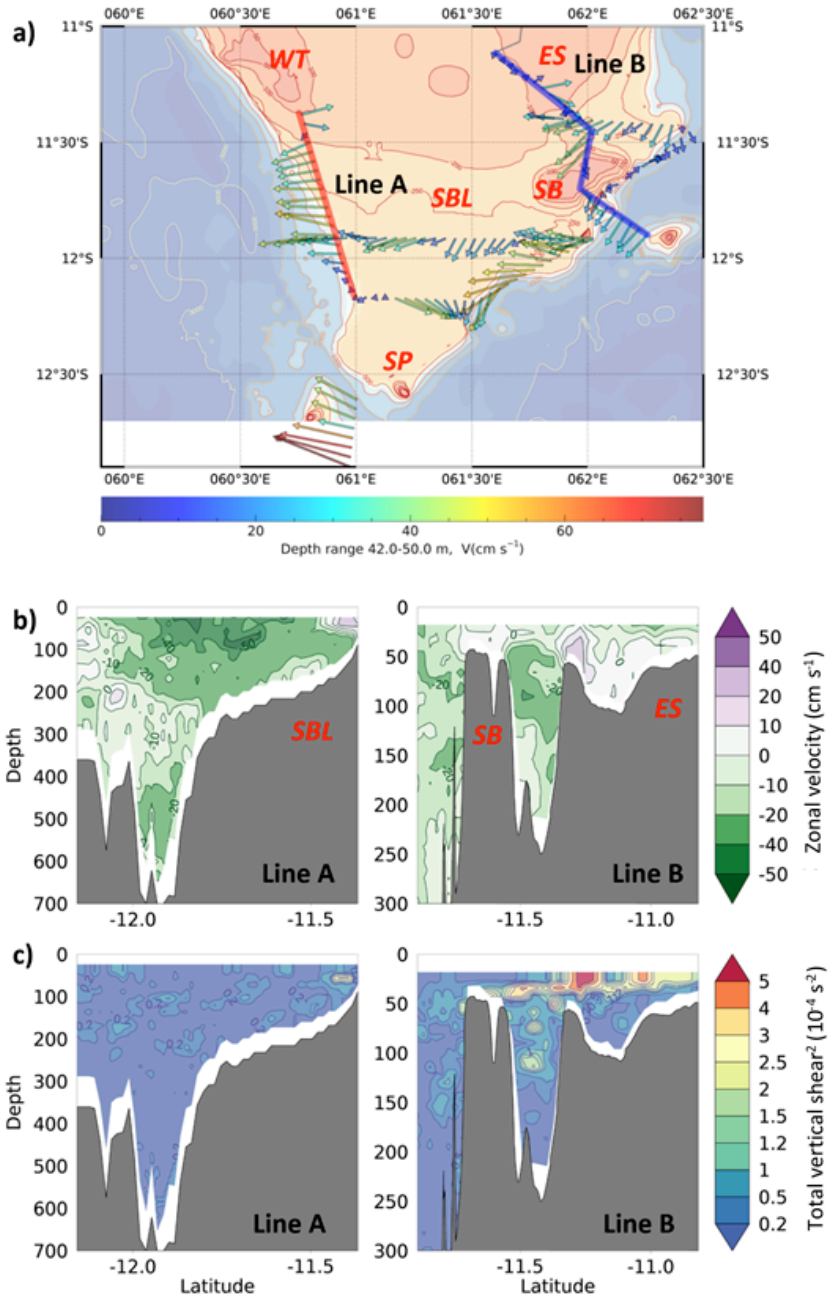

Figure 6. Distributions of ADCP-derived currents over the southern section of the Saya de Malha bank for: a) Horizontal currents (cm s^{-1}) observed in the 42-50 m layer; (b) Vertical distribution of the zonal velocity component (cm s^{-1}) computed from Line A (left) and Line B (right); and c) Total vertical shear squared distribution of horizontal velocity (10^{-4} s^{-2}) computed from Line A (left) and Line B (right).

hypothesis of the recirculation current pattern in the Central Lagoon region. By way of validation, the total SEC transport across the SN sill was computed, the region that was covered immediately after completing the observations over SDM (on 27 May). The result, using the 75 kHz ADCP (depth range 800 m) yielded 20.3 Sv, comparing well to previous studies with 23 Sv obtained from Lowered-ADCP (New *et al.*, 2007) and 14.41 Sv from ADCP 150 kHz (depth range 300 m) (Vianello *et al.*, 2017).

Vertical shear

Figure 6c presents the distribution of the vertical shear squared (Sh^2) of the horizontal velocity observed across Lines A and B. On the downstream of the SEC (Line A), the entire water column displayed a low shear ($< 1 \times 10^{-4}$ s^{-2}), manifesting a vertically rigid flow. On the upstream side (Line B), the vertical rigidity was confined to the deeper part (south of the SB). The Sh^2 increased visibly north of the SB, over the parts of the section characterized by the abrupt and shoaling topography.

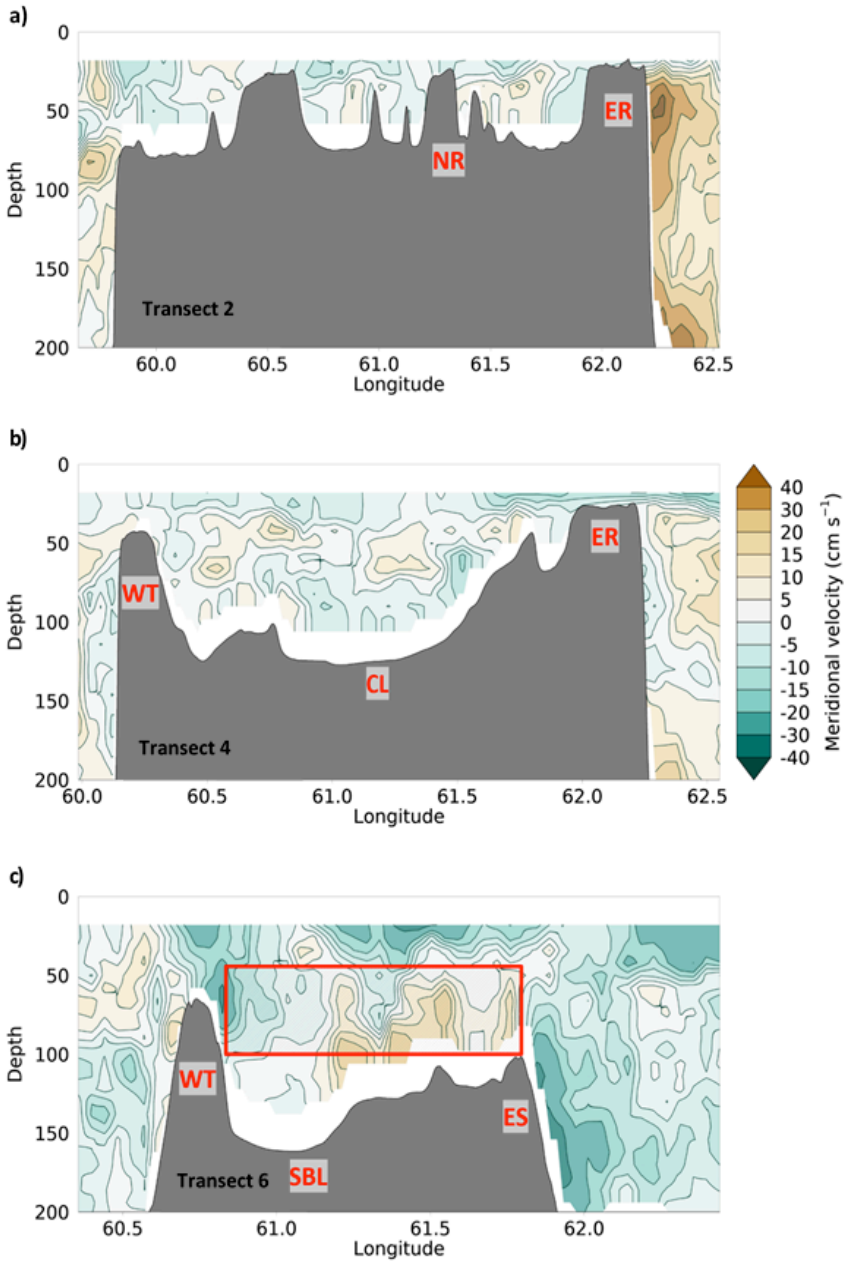

Figure 7. Meridional velocity (cm s^{-1}) component observed along the transect lines characteristic to the bathymetric regions of the Saya de Malha Bank for: a) Transect 2 – Northern Rim (NR); b) Transect 4 – Central Lagoon (CL); and c) Transect 6 – Shelf Break Ledge (SBL; the red box delimits the area used for the computation of volume transport in this region).

Strong shear (> 3 x 10^{-4} s^{-2}) was observed throughout this region, confined to the thermocline depth. However, the vertical shear tended to be more enhanced and expanded vertically over elevated topographic features of the bank. The vertical shear distribution pattern presented here characterized most of the ADCP data collected over slopes and the Central Lagoon (not shown). Strong shear was absent over the shallowest regions (NR and ER), coincident with the absence of stratification and TSW present near-bottom.

Discussion

This paper investigated the effect of the shallow bathymetry of SDM on the large circulation pattern of the SWIO; that is the westward propagating SEC, and consequently the down-scaled current pattern developed over the bank. The results presented in the previous section were congruent with the literature on the wind regime (southeast trade winds) established in the SWIO, leading to a westward propagating current, the SEC, and the topographic steering of the SEC along the slopes of the bank, resulting in the divergence of the SEC, feeding the northern and southern part of SDM. The surface current pattern was found to follow the wind-induced Ekman transport across the bank, flowing in a generally southwestward direction (10-20 cm/s) with increasing intensity in the southern region of the bank (40-50 cm/s). Moreover, the study revealed a two-layer structure of the current over the shallow bank; the top layer characterizing the TSW transport and the sub-thermocline layer appearing to recirculate over the central region of the bank. This two-layered current pattern was further corroborated by the vertical shear and volume transport analyses over the SDM region.

The mountainous-like topography of SDM clearly demonstrates the possibility of Internal Solitary Waves (ISWs) forming due to flow-topography interactions which are common occurrences in oceanography (Xie *et al.,* 2017). ISWs have been found to propagate over the SDM region and appeared to be originating from multiple sources which are generated by semi-diurnal tides, on both the western and southern slopes of the bank (New *et al*., 2013). Lee ISWs have also been observed at the SN sill and are considered as one of the largest known in the world (Konyaev *et al*., 1995; da Silva *et al*., 2011, New *et al*., 2013; da Silva *et al*., 2015). Packets of large ISWs propagating towards both a west-northwest and east-southeast direction from the SN sill near 12.5°S were recorded (da Silva *et al*., 2011). In the light of the findings on the role of tidal current and internal waves in the current dynamics of SDM (New *et al*., 2013; da Silva *et al*., 2015; da Silva *et al*., 2011), the hypothesis of a recirculating current in the sub-thermocline layer over the Central Lagoon may be oversimplified given the ISWs conditions established over the bank region.

A significant proportion of baroclinic tides propagate in a northeast direction (New *et al.*, 2013); thus over the region marked as SBL in this investigation. The activity of these wave packets explains large differences in the depth of the thermocline observed at the CTD stations occupied in this region (Stations 414, 410 and 406, Fig. 3). The prevailing northeast propagation direction implies that the shoaling eastern slope is the place for intense ISW breaking, therefore the location of strong turbulence, nutrient fluxes and, as New *et al.* (2013) pointed out, enhanced biological productivity. Furthermore, as the internal wave breaking induces longshore currents along isobaths (Zikanov and Slinn, 2001), the recirculation observed in Figure 5b is probably a manifestation of such currents.

The SEC is known to form a sharp boundary between the subtropical water masses from further north (nutrient-rich waters) and south (nutrient-poor waters) of the bank (New *et al*., 2007; Vortsepneva, 2008). The T/S profiles presented in New *et al.* (2007) showed little variations across the east-west profiles as compared to the north-south profiles. This could indicate that the topography along with the current dynamics enhance the mixing of water masses over the shallow bank (Pous *et al*., 2014). Additionally, this paper showed that the interaction of water masses with the bank differs strikingly. The TSW flows with the westward-flowing current (SEC) while the underlying STSW moves in a northward direction from the South Point and further interacts with the topography of the bank, establishing local oceanographic conditions. The pycnocline fluctuated strongly between Stations 414 to 406, manifesting the amplified ISW activity near the shelf-break as New *et al.* (2013) predicted. Underlying the pycnocline, water masses identified as ITW and STSW were present (New *et al.,* 2007; Vianello *et al.*, 2017). In the region of the topographically steered SEC flow, along the southern slope, the distributions of all three seawater properties were identical to those characterizing the SEC region upstream of the plateau (e.g. New *et al.*, 2007, in their Fig. 11 to 13]. The current dynamics such as the formation and propagation of ISWs over the shallow bank therefore plays a significant role in the distribution and mixing of water masses.

In the collected datasets, semi-diurnal tidal signal and minute-scale fluctuations from ISW motions were detected in both the ADCP and CTD analyses. For example, it was not unusual to observe a rise or fall of the thermocline by 40 m at the time of a CTD cast. However, to account for these tidally induced motions was beyond the scope of the observational programme adopted for this research survey. Further in-depth studies are therefore required to assess the role of the current dynamics developing over the shallow bank region.

Conclusion

This study provided a first synoptic outline of the current pattern developed over the shallow SDM resulting from the interaction of the SEC with the topography of the bank. The main observations derived from the ADCP and CTD datasets collected during the survey over the SDM are: (1) the vertically rigid flow over the southern slopes exposed to the SEC throughflow contrasting with the two-layered flow structure over the inner bank; (2) the top layer carrying the water mass, TSW, driven by the Ekman dynamics; as opposed to the (3) sub-thermocline currents, most likely controlled by the tidal and internal wave dynamics.

Acknowledgements

The underlying work was made possible with the support of the EAF-Nansen Programme "Supporting the Application of the Ecosystem Approach to Fisheries Management considering Climate Change and Pollution Impacts" executed by Food and Agriculture Organization of the United Nations (FAO) and funded by the Norwegian Agency for Development Cooperation (Norad). The authors are thankful to the FAO for funding and supporting the Indian Ocean research expedition 2018 (NORAD-FAO PROJECT GCP/INT/730/NOR) on the Saya de Malha Bank on board the R/V Dr Fridtjof Nansen. The authors are grateful to the Department for Continental Shelf, Maritime Zones Administration & Exploration (Prime Minister's Office, Republic of Mauritius) for coordinating and co-leading the expedition and for their continuous support towards the publication of this research study, and the Mauritius-Seychelles Joint Commission of the Extended Continental Shelf for their support and assistance and granting the necessary authorisations. Ms J Ramma is gratefully acknowledged for her contribution in collecting and conducting pre-analysis work of the physical oceanography data during the expedition. The authors are thankful to the participants of the expedition and the crew members for their work and contribution during the 2018 expedition cruise.

References

Bergstad OK, Bissessur D, Sauba K, Rama J, Coopen P, Oozeeraully Y, Seeboruth S, Audit- Manna A, Nicolas A, Reetoo N, Tabachnick K, Kuyper D, Gendron G, Hollanda S, Melanie R, Souffre A, Harlay J, Bhagooli R, Soondur M, Ramah S, Caussy L, Ensrud TM, Olsen M, Høines ÅS (2020) Regional resources and ecosystem survey in the Indian Ocean, Leg 2.1. Characterizing ecosystems and morphology of the Saya de Malha Bank and Nazareth Bank, 3 May - 4 June 2018. NORAD-FAO Programme GCP/GLO/690/NOR, Cruise reports Dr Fridtjof Nansen, EAF-Nansen/CR/2018/6.

Bergstad OK, Tabachnick K, Rybakova E, Gendron G, Souffre A, Bhagooli R, Ramah S, Olsen M, Høines SA, Dautova T (2021) Macro- and megafauna on the slopes of the Saya de Malha Bank of the Mascarene Plateau. Western Indian Ocean Journal of Marine Science, Special Issue 2/2021: 129-158

Cancet M, Griffin D, Cahill M, Chapron B, Johannessen J, Donlon C (2019) Evaluation of GlobCurrent surface ocean current products: A case study in Australia. Remote Sensing of Environment 220: 71-93 [doi:https://doi.org/10.1016/j.rse.2018.10.029]

Commission on the Limits of the Continental Shelf (CLCS) (2011) Summary of the recommendations of the commission on the limits of the continental shelf in regard to the joint submission made by Mauritius and Seychelles concerning the Mascarene Plateau region on 1 December 2008, CLCS/70 (11 May 2011). United Nations. 19 pp

Cushman-Roisin B, Beckers JM (2011) Introduction to geophysical fluid dynamics: physical and numerical aspects. Academic press. 875 pp

da Silva JCB, New AL, Magalhaes JM (2011) On the structure and propagation of internal solitary waves generated at the Mascarene Plateau in the Indian Ocean. Deep Sea Research, Part I: Oceanographic Research Papers 58 (3): 229-240 [doi:https://doi.org/10.1016/j.dsr.2010.12.003]

da Silva JCB, Buijsman MC, Magalhaes JM (2015) Internal waves on the upstream side of a large sill of the Mascarene Ridge: a comprehensive view of their generation mechanisms and evolution. Deep Sea Research Part I, 99: 87-104 [doi: 10.1016/j.dsr.2015.01.002]

Fischer J, Brandt P, Dengler M, Müller M, Symonds D (2003) Surveying the upper ocean with the ocean surveyor: a new phased array doppler current profiler. Journal of Atmospheric and Oceanic Technology 20: 742-751

Genin A (2004) Bio-physical coupling in the formation of zooplankton and fish aggregations over abrupt

topographies. Journal of Marine Systems 50 (1-2): 3-20 [doi:10.1016/j.jmarsys.2003.10.008]

Kara VI, Sivukha NM (1990) Marine geology: Geomorphology and recent development of the Central Mascarene Ridge. Oceanology 30 (2): 303-308

Konyaev KV, Sabinin KD, Serebryany AN (1995) Large-amplitude internal waves at the Mascarene Ridge in the Indian Ocean. Deep Sea Research, Part I: Oceanographic Research Papers 42 (11-12): 2075-2091

Langdon C, (2010) Determination of dissolved oxygen in seaweater by Winkler titration using amperometric technique. In: Hood EM, Sabine CL, Sloyan BM (eds) The GO-SHIP repeat hydrography manual: A collection of expert reports and guidelines, Version 1. 18 pp [doi: https://doi.org/10.25607/OBP-1350]

Lindhorst S, Appoo J, Artshwager M, Bialik O, Birkicht M, Bissessur D, Braga J, Budke L, Bunzel D, Coopen P, Eberhardt B, Eggers, D Eisermann JO, El Gareb F, Emeis K, Geßner A-L, Hüge F, Knaack-Völker H, Kornrumpf N, Lenz N, Lüdmann T, Metzke M, Naderipour C, Neziraj G, Reijmer J, Reolid J, Reule N, Rixen T, Saitz Y, Schäfer W, Schutter I, Siddiqui C, Sorry A, Taphorn B, Vosen S, Wasilewski T, Welsch A (2019) SONNE-Berichte, Saya de Malha Carbonates, Oceanography and Biogeochemistry (Western Indian Ocean). Cruise No. SO270, MASCARA (BMBF grant 03G0270A). 102 pp [https://doi.org/10.2312/cr_so270]

New AL, Stansfield K, Smythe-Wright D, Smeed DA, Evans AJ, Alderson SG (2005) Physical and biochemical aspects of the flow across the Mascarene Plateau in the Indian Ocean. Philosophical Transactions of the Royal Society A 363: 151-168 [doi: 10.1098/rsta.2004.1484]

New AL, Alderson S, Smeed D, Stansfield K (2007) On the circulation of water masses across the Mascarene Plateau in the South Indian Ocean. Deep Sea Research, Part I 54 (1): 42-74 [doi: 10.1016/j.dsr.2006.08.016]

New AL, Magalhaes JM, da Silva JCB (2013) Internal solitary waves on the Saya de Malha bank of the Mascarene Plateau: SAR observations and interpretation. Deep Sea Research, Part I 79: 50-61 [doi: 10.1016/j.dsr.2013.05.008]

Ostrowski M, da Silva JCB, Bazik-Sangolay B (2009) The response of sound scatterers to El Nino- and La Nina-like oceanographic regimes in the southeastern Atlantic. ICES Journal of Marine Science 66 (6): 1063-1072 [doi:https://doi.org/10.1093/icesjms/fsp102]

Payet R (2005) Research, assessment and management on the Mascarene Plateau: a large marine ecosystem perspective. Philosophical Transactions of the Royal Society A: Mathematical, Physical and Engineering Sciences 363 (1826): 295-307 [doi:10.1098/rsta.2004.1494]

Pous, S, Lazure P, Andre G, Dumas F, Halo I, Penven P (2014) Circulation around La Reunion and Mauritius islands in the south-western Indian Ocean: A modeling perspective. Journal of Geophysical Research: Oceans 119: 1957-1976 [doi:10.1002/2013JC009704]

Ramah S, Gendron G, Bhagooli R, Soondur M, Souffre A, Melanie R, Coopen P, Caussy L, Bissessur D, Bergstad OK (2022) Diversity and distribution of the shallow water (23 – 50 m) benthic habitats in the Saya de Malha Bank, Mascarene Plateau. Western Indian Ocean Journal of Marine Science, Special Issue 2/2021: 69-80

Schott FA, McCreary JP (2001) The monsoon circulation of the Indian Ocean. Progress in Oceanography 51 (1): 1-123 [doi: 10.1016/S0079-6611(01)00083-0]

Schott FA, Xie SP, McCreary JP (2009) Indian Ocean circulation and climate variability. Reviews of Geophysics 47 (1). 46 pp

Stømme T, Bjordal Å, Ansorge I, Balarin E, Ostrowski M, Francourt H, Bornman T, Plos A, Gibbons M, Cedras R, Bernard K, Kaehler S, Hill J, du Plessis S, Scott L, Tweddle D, Palmer R, Govinden R, Lucas V, Etienne M, McPhaden M, Kunze S, O'Donaghue K, Alvheim O, Zaera D, Mørk T, Sverre Fossheim O (2009) 2008 ASCLME Survey No 3, Cruise report No 7/2008, 8 October – 27 November 2008. Report No. EAF-N2008/7. Institute of Marine Research Bergen, Norway. 96 pp

Vianello P, Ansorge IJ, Rouault M, Ostrowski M (2017) Transport and transformation of surface water masses across the Mascarene Plateau during the Northeast Monsoon season. African Journal of Marine Science 39 (4): 453-466 [doi: 10.2989/1814232X.2017.1400999]

Vortsepneva E (2008) Saya de Malha Bank – an invisible island in the Indian Ocean. Geomorphology, oceanology, biology. Lighthouse Foundation. 44 pp

Xie X, Li M, Scully M, Boicourt WC (2017) Generation of internal solitary waves by lateral circulation in a stratified estuary. Journal of Physical Oceanography 47 (7):1789-1797

Zeng Z, Brandt P, Lamb KG, Greatbatch RJ, Dengler M, Claus M, Chen X (2021) Three-dimensional numerical simulations of internal tides in the Angolan upwelling region. Journal of Geophysical Research: Oceans 126 (2): p.e 2020JC016460

Zikanov O, Slinn D (2001) Along-slope current generation by obliquely incident internal waves. Journal of Fluid Mechanics 445: 235-261 [doi:10.1017/S0022112001005560]